Research Article

Molecular Interaction Studies of Amorphous Solid Dispersions of the Antimelanoma Agent Betulinic Acid

Meiki Yu,[1] Joseph E. Ocando,[2] Louis Trombetta,[1] and Parnali Chatterjee[1,3]

Abstract. Betulinic acid (BA), a novel natural product with antimelanoma activity, has poor aqueous solubility (<0.1 µg/mL) and therefore exhibits poor bioavailability. The purpose of this study was to explore the feasibility of preparing BA solid dispersions (BA-SDs) with hydrophilic polymers to enhance the aqueous solubility of BA. Melt-quenched solid dispersions (MQ-SDs) of BA were prepared at various ratios with the hydrophilic polymers including Soluplus, HPMCAS-HF, Kollidon VA64, Kollidon K90, and Eudragit RLPO. BA was found to be miscible in all polymers at a 1:4 (*w/w*) ratio by modulated differential scanning calorimetry (MDSC). BA/Soluplus MQ-SD exhibited the highest solubility in simulated body fluids followed by BA/Kollidon VA64 MQ-SD. The MQ-SDs of BA/Soluplus, BA/HPMCAS-HF, and BA/Kollidon VA64 were found to be amorphous as indicated by X-ray powder diffraction (XRPD) studies. Fourier transform infra-red (FT-IR) studies indicated molecular interactions between BA and Soluplus. Our preliminary screening of polymers indicates that Soluplus and Kollidon VA64 exhibit the greatest potential to form BA-SDs.

KEY WORDS: betulinic acid; DSC; FT-IR; HPLC; SEM; solid dispersions; solubility; XRPD.

INTRODUCTION

Betulinic acid (3β-hydroxy-lup-20(29)-en-28-oic acid) is a novel pentacyclic lupane-type triterpene (Fig. 1) obtained from the outer bark of *Betula alba* and many other plants (1). Betulinic acid (BA) and its derivatives have been reported to be cytotoxic against melanoma, neuroblastoma, ovarian, lymphoma, lung, and cervical cancer cell lines and *in vivo* (2–6). The antitumor activity of BA is mediated by the induction of apoptosis through alterations in the mitochondrial membrane potential and the generation of ROS (7,8). Because of its high antitumor activity and lack of toxicity, BA is currently under phase II clinical trials for the treatment or prevention of dysplastic melanocyte nevi as a 20% BA ointment (9). Apart from its antimelanoma activity, it is known to inhibit human immunodeficiency virus (HIV) replication in H9 lymphocyte cells, block HIV-1 entry into cells, and inhibit DNA polymerase (10,11). To date, numerous derivatives of BA have been synthesized as maturation inhibitors of HIV-1,

with Bevirimat (i.e., PA-457 or 3-*O*-(3′,3′-dimethylsuccinyl)) derivative of BA (11) being the most promising new chemical entity (NCE). Bevirimat is a first-in-class HIV virus maturation inhibitor that has shown a substantially greater therapeutic response (therapeutic index >2,500) compared to that of BA against HIV virus maturation (11). In spite of an excellent therapeutic index, the phase IIb clinical trial of Bevirimat has been discontinued due to the poor response of patients to the drug.

One reason for the failure of BA and its derivatives in the clinical trials is its poor aqueous solubility (0.02 µg/mL; (12)). Therefore, improving the apparent aqueous solubility of BA is pertinent for its advancement through the clinical development process. Numerous groups have reported the development of various BA formulations, including the complexation of BA with cyclodextrin (13–15), nanoemulsions (16,17), and liposomes (5,18), to enable preclinical studies of BA; however, none have demonstrated the ability to substantially improve the bioavailability of BA.

To the best of our knowledge, amorphous solid dispersion as a strategy to improve the apparent solubility of BA has not yet been explored. The ability of amorphous solid dispersions to improve the dissolution rate and enhance the bioavailability of BCS class II and IV drugs has been well established in the literature (19–21). Solid dispersion refers to the dispersion of one or more drugs in a polymeric matrix/carrier in the solid state, which can yield a eutectic (i.e., a non-molecular level of mixing) or a solid solution (i.e., molecular-level mixing) product (22–24). Because amorphous solid dispersions have higher internal energy and enhanced molecular mobility, they have a

[1] Department of Pharmaceutical Sciences, St. John's University, 8000 Utopia Pkwy, Queens, NY 11439, USA.
[2] Department of Chemistry, St. John's University, 8000 Utopia Parkway, Queens, New York 11439, USA.
[3] To whom correspondence should be addressed. (e-mail: chatterp@stjohns.edu)
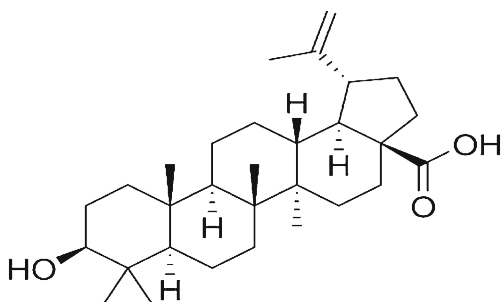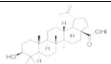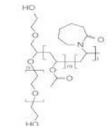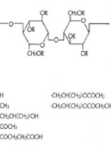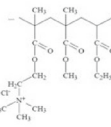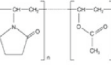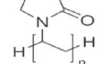
Fig. 1. Chemical structure of betulinic acid

greater propensity to convert to the thermodynamically more stable crystalline form during the manufacturing process and storage (25). One of the preferred methods to stabilize the amorphous state of a drug is to prepare solid polymer dispersions (20) by either melting (hot melt extrusion, thin film cooling, melt quench, milling), solvent evaporation (oven drying, rotary evaporation, spray drying, co-precipitation, or electrostatic spinning), or melting solvent method (26). In this study, we implemented the melt-quench (MQ) method in order to prepare solid dispersions of BA.

Although polymeric solid dispersions of drugs have been shown to significantly improve the physical stability of the amorphous drug substance, the mechanism by which polymers stabilize the amorphous solid is not completely understood nor is the method by which appropriate polymers that can be selected for a particular drug substance known. Many theories have been proposed, but the most plausible explanation is that polymers increase the Tg of the drug substance thereby retarding the molecular mobility of the amorphous drug and inhibiting the crystallization process (19,27,28). If the storage temperature is such that it is close to or higher than the Tg of the amorphous substance, the glassy solution can be converted to a rubbery form and lead to the crystallization of the amorphous material (29). In addition to the temperature, the presence of moisture or water, the method by which amorphous solid dispersions are prepared, the amount of drug that is loaded, the miscibility of the drug-polymer mixture, and whether a high Tg can be achieved, collectively can enhance the molecular mobility of the drug-polymer mixture causing nucleation and recrystallization of the amorphous drug product, which can impact the dissolution rate and the wettability of the drug such that a supersaturated state of the drug may not be maintained for a prolonged time period at the site of absorption (25). Drug substances that exhibit higher crystallization enthalpy and lower nucleation activation energy have a greater tendency to crystallize. For a polymer to increase the Tg of the drug, the drug-polymer mixture must be thermodynamically miscible and homogenous, have a high Tg, negative free energy, negative enthalpy, and be physically stable such that it does not transform to the crystalline state (30). There are a number of techniques available to evaluate the miscibility and the stability of the amorphous solid dispersions. In this study, differential scanning calorimetry (DSC, which detects the presence of a single Tg) and X-ray powder diffraction (XRPD, a widely accepted tool for evaluating the physical stability of the drug-polymer mixture) were utilized to investigate the feasibility of preparing amorphous solid polymer dispersions of BA by dispersing BA in different polymers using the MQ method with the objective of improving the apparent solubility of BA.

There are numerous examples in the literature where the MQ method has been used at early development stage to screen polymers for their ability to be miscible with the drug substance (31–33). Despite melt extrusion being the most popular method for preparing large-scale amorphous solid dispersions (easy adaptability, reduced solvent use, reduced cost, and the ability for continuous processing), lab-scale melt extrusion requires large quantities of drug substance which is generally not available at the early developmental stages, especially in this study. BA is a novel natural product that is isolated from the outer bark of plants and trees; therefore, large quantities of BA are not commercially available. Hence, the MQ method was adapted for the present pilot-scale feasibility study for screening polymers in order to prepare amorphous solid dispersions of BA.

The hydrophilic polymers Soluplus, HPMCAS-HF, Kollidon VA 64, and Kollidon K90 used in our study were selected on the basis of their ability to maintain supersaturation of drugs in the gastrointestinal tract by inhibiting nucleation and crystallization of the drug and enhancing the dissolution of poorly water-soluble new chemical entities (Table I). Soluplus is an amphiphilic polyvinylcaprolactam polyvinylacetate polyethylene glycol graft copolymer that can form solid solutions and improve the solubility and bioavailability of poorly water-soluble drugs (35). The polyvinylcaprolactam and polyvinylacetate groups form the lipophilic part of the polymer whereas the hydrophilic backbone is composed of polyethylene glycol (PEG 6000). Soluplus can function as a polymer matrix for solid solutions and as a solubilizer for water-insoluble drugs, which makes it suitable for melt extrusion of poorly water-soluble drugs. Kollidon K90 (PVP K90) is obtained by free radical polymerization of vinylpyrrolidone whereas Kollidon VA64 (PVP VA64) is manufactured by the polymerization of N-vinylpyrrolidone and vinylacetate. The PVP polymers have carbonyl (−C=O) functionality in their structure which can hydrogen bond with drugs that contain a proton donor and stabilize amorphous drug substances (36). Hypromellose acetate succinate (HPMCAS-HF) is a cellulose-based enteric coating polymer with hydroxypropoxy, methoxy, acetyl, and succinoyl substitutions (Table I) that prevents the dissolution of certain drugs in the acidic milieu of the stomach, thus avoiding the degradation of the drug in stomach pH (37). In addition, amorphous solid dispersions containing HPMCAS are more effective than Kollidon VA64 and K90 polymers in maintaining supersaturation of the drugs in the gastrointestinal environment by inhibiting nucleation and crystallization of the drug due to the presence of carboxylic acid groups (38–40). The hydroxyl groups in HPMCAS can form hydrogen bonds with electronegative groups such as oxygen and nitrogen in drug molecules and enhance the solubility of the poorly water-soluble drugs. Although HPMCAS has great potential in enhancing the solubility of poorly water-soluble drugs, it can undergo hydrolysis at high temperature during manufacturing and release acetic acid and succinic acid which can react with the hydroxyl groups in the active pharmaceutical ingredient (API) and form esters thereby causing drug-excipient incompatibilities. Eudragit RLPO is an insoluble ethyl acrylate and methyl methacrylate copolymer with a low percentage of methacrylic acid ester with quarternary ammonium groups. It is capable of swelling which is independent of the physiological pH and is usually included as a

Table I. Chemical Properties/Functions of Polymers

Compound	Structural Formula	Molecular Weight	Degradation Temperature	Properties
Betulinic Acid		456.7 g/mol	NA	Poor solubility in most solvents (Jäger *et al.* 2007), permeability not reported in literature yet
Soluplus		90,000 – 140,000 g/mol	250ºC	Solubilizer for poorly soluble drugs in aqueous media (Hardung *et al.* 2010)
HPMCAS-HF		17,000 – 20,000 g/mol	NA	Solubilization of poorly soluble APIs (Ray 2010), ability t o maintain drug supersaturation in GI milieu (Curatolol 2009)
Eudragit RLPO		~32,000 g/mol	NA	Time-controlled release, pH-independent swelling, insoluble, high permeability (Envonik)
Kollidon VA 64		45,000 – 70,000 g/mol	230ºC	Plasticity, excellent dry binders for direct compression and roller compaction, binder for wet granulation, film forming agent in tablet coating/cubcoating as well as topical sprays (BASF, 2011)
Kollidon K90		360,000 g/mol	200ºC	Suspension stabilizer, solubilizer, binder, capability to form hydrogen bonds with compounds with complementary structures for improved dissolution (Buhler 1998; Folttmann 2008))

NA not available, *HPMCAS-HF* hypromellose acetate succinate

carrier to design controlled release delivery systems (Evonik). Since BA is a poorly water-soluble drug, the inclusion of a polymer such as Eudragit RLPO can produce sustained release of BA and enhance the dissolution and bioavailability of the drug.

Based on the differential ability of the polymer excipients to enhance the dissolution of poorly water-soluble new chemical entities, through this study, we sought to elucidate the (1) thermodynamic properties of BA, (2) the solubility (or the miscibility) of BA in five pharmaceutical polymers by modulated DSC (MDSC) and HPLC, and (3) the solid state and chemical state of BA/polymer mixtures (XRPD, SEM, and Fourier transform infra-red (FT-IR)) in order to improve the aqueous solubility of BA. The miscibility of the BA-polymer mixtures was investigated by MDSC, XRPD, SEM, and HPLC and by comparing the experimentally obtained Tg of the MQ-BA-polymer samples with the predicted Tg using the Fox equation. The intermolecular interactions (such as hydrogen bonding) between BA and the polymers were evaluated by FT-IR. Finally, the solubility of the MQ-BA-polymer samples was determined by HPLC.

MATERIALS AND METHODS

Materials

Betulinic acid was obtained from Enzo Life Sciences (USA). Soluplus, Kollidon VA64, and Kollidon K90 were donated by BASF (USA). HPMCAS-HF was obtained from Shin-Etsu Chemical Co. (USA), and Eudragit RLPO was a gift from Evonik (USA). Polyvinylidene difluoride (PVDF) filters (0.45 μm) were purchased from EMD Millipore (USA). T-zero pans and lids were procured from TA Instruments (USA). Methanol and acetonitrile were purchased from EMD Chemicals (USA). Acetic acid was purchased from Fisher Scientific (USA). All other chemicals were of high purity or analytical grade and used as received.

Methods

Preparation of Physical Mixtures of BA and Polymer and BA/ Polymer Melt-Quenched Samples (MQ-SD)

Physical mixtures (PMs) of BA-polymers were prepared by gently grinding accurately weighed BA and respective polymer (Table I) at BA/polymer ratios of 2:1, 1:1, 1:2, and 1:4 (*w/w*) for 2–3 min in a pestle and mortar. BA/polymer MQ-SD were prepared by accurately weighing approximately 5 mg of the BA/polymer physical mixture at different ratios on T-zero aluminum pans and hermetically sealed with T-zero aluminum lids. The samples were then heated to 200°C at a rate of 10.0°C/min modulated at ±1°C every 60 s, isothermed for 5 min to reduce the presence of adsorbed water, and then rapidly cooled (quench cooled) to −10°C at a rate of 50.0°C/min followed by a 5-min isothermal treatment. An empty pan was used for reference and the instrument was calibrated regularly with indium. The obtained samples were designated as melt-quenched samples (MQ-SDs).

Solid-State Characterization of BA, the PM, and the MQ-SD

Modulated Differential Scanning Calorimetry. The thermal properties of BA, the PMs, and the MQ-SDs were characterized using modulated differential scanning calorimetry (TA Instruments, model DSC Q200). Neat BA was heated to 200°C at a rate of 10.0°C/min modulated at ±1°C every 60 s, isothermed for 5 min to reduce the presence of adsorbed water, and then heated to 350°C at a rate of 10.0°C/min modulated at ±1°C every 60 s. The PMs and MQ-SDs were heated to 350°C at a rate of 10.0°C/min modulated at ±1°C every 60 s.

X-ray Powder Diffraction. Solid-state characterization of BA and the MQ-SD was performed by X-ray powder diffraction (XRPD) analysis at ambient temperature, where samples were loaded onto a 0.3-mm Hampton Nylon loop for measurements. X-ray data were collected on a Bruker D8 DISCOVER GADDS microdiffractometer equipped with a VÅNTEC-2000 area detector. The X-rays generated from a sealed Cu tube were monochromated by a graphite crystal and were collimated by a 0.5-mm MONOCAP (λ Cu-$K\alpha$=1.54178 Å). The sample-to-detector distance was 150 mm. Data were merged and integrated using the XPRD2EVAL program in the Bruker PILOT software package (PILOT, version 2009.5-0, program for Bruker D8 DISCOVER X-ray diffractometer control, Bruker AXS, Madison, WI). The raw file was analyzed using the Jpowder data visualizer software (DIFFRAC^{plus} EVA (version 15) software package for powder diffraction, Bruker AXS, Madison, WI).

Scanning Electron Microscopy. The surface morphologies of BA, the polymers, and the MQ-SDs were assessed using a scanning electron microscope (JSM-6010LA, Joel Analytical Scanning Electron Microscope, MA, USA). A small amount of the sample was fixed onto an aluminum stud with a double-sided conductive lift-n-press adhesive tab (Electron Microscopy Sciences, PA, USA). A very thin layer of platinum was deposited onto the sample by a sputtering unit operated at 20 mA for 4 min (EMS 550X Sputter Coater, Electron Microscopy Sciences, PA, USA). The platinum-coated samples were placed in the microscope chamber, and a high vacuum was applied to evacuate the specimen chamber. Micrographs were captured at various magnifications such that the morphology could be visualized.

Attenuated Total Reflection Fourier Transform Infra-red Spectroscopy. Molecular interactions between BA and the polymers were characterized using a FT-IR spectrometer equipped with a universal attenuated total reflection (ATR) accessory (PerkinElmer Spectrum 100). A small amount of each sample was placed in the ATR cell, and pressure was applied with a pressure arm. Scans were collected in the range of 4,000–700 cm^{-1} using the Spectrum software package (PerkinElmer, MA, USA).

Chemical Analysis of BA in the MQ-SD

The concentration of BA in the MQ-SDs was evaluated using an Agilent 1100 HPLC. Neat BA (pre- and post-MQ treatment) and the PM were used as controls. An isocratic method of 10% mobile phase A (0.1% acetic acid in deionized water) and 90% mobile phase B (0.1% acetic acid in acetonitrile) at a flow rate of 1.0 mL/min was used to determine the concentration of BA, with a run time of 6 min and an injection volume of 60–100 μL. The column used was an Agilent Eclipse Plus C18 (4.6 mm×100 mm, 3.5 μm) at a detection wavelength of 210 nm. All of the experiments were conducted in triplicate. The data are represented as the means ± standard deviation (SD) of n=3.

The BA/polymer MQ-SD degradation profile was evaluated using a gradient method on an Agilent 1100 HPLC. Neat BA (pre- and post-MQ treatment) and the PM were used as controls. A gradient method consisting of 0.1% acetic acid in deionized water as mobile phase A and 0.1% acetic acid in acetonitrile as mobile phase B was used at a flow rate of 1.0 mL/min with a run time of 30 min and an injection volume of 30–60 μL. The column used was an Agilent Eclipse Plus C18 (4.6 mm×100 mm, 3.5 μm) at a detection wavelength of 210 nm. All of the experiments were conducted in triplicate. The data are represented as the means ± SD of n=3.

Solubility Studies of the MQ-SDs

The solubility profiles of BA and the MQ-SDs at 1:4 (*w/w*) ratio together with the PMs at the same ratio were dispersed in simulated gastric fluid (SGF) and simulated intestinal fluid (SIF) at a concentration equivalent to 1 mg/mL of BA. The samples were shaken for 24 h at 37°C on a shaker (VWR Symphony incubating microplate shaker), and the solubility was determined by HPLC after the samples were filtered through 0.45-μm PVDF filters followed by dilution with an appropriate diluent. All of the experiments were conducted in triplicate. The data are represented as the means ± SD of n=3.

RESULTS

Physico-Chemical Characterization of Neat BA

The melting temperature (*Tm*) and the glass transition temperature (*Tg*) of neat BA was found to be ~321.4 and ~119.8°C, respectively (Fig. 2). Active pharmaceutical ingredients (APIs) that demonstrate good glass-forming properties have *Tg*/*Tm* (in Kelvin) ratio greater than 0.67 (i.e., the rule of 2/3rds) according to the Boyer-Beaman rule (41) in order to form solid dispersions. In the case of BA, the *Tg*/*Tm* ratio is estimated to be 0.66 which is slightly less than the rule of 2/3rds, indicating that BA may still be able to form solid dispersions. The presence of sharp peaks in the XRPD pattern of neat BA confirmed the crystalline nature of the drug (Fig. 3). The SEM image of neat BA appears rod-like with the particle size in the sub-micron (20 μm) range (Fig. 4 (i)). The SEM image of the MQ sample of BA after the first and second heating cycles (Fig. 4 (iii–iv)) appears spongy and powdery with the loss of the rod-like structure seen with neat BA (Fig. 4 (i)). The FT-IR spectrum of BA (Fig. 5a) contained characteristic bands at 3,400 cm^{-1} that corresponded to the O-H stretching of the hydroxyl group at C-3 position in BA, 2,945 cm^{-1} that is indicative of C–H stretching, 1,701 cm^{-1} that corresponded to the C=C stretching of the ethylene side chain, 1,684 cm^{-1} that is indicative of the C=O stretching of the carboxylic acid at C-28 position in BA, and 1,432 cm^{-1} that corresponded to the CH$_3$ bending of the methyl groups in BA. The solubility of neat BA (Table II) was found to be below the

limits of detection by HPLC (<0.2 μg/mL) in simulated gastric fluid (SGF) but was found to be approximately ninefold higher (1.8 μg/mL) in simulated intestinal fluid (SIF). Based on these physico-chemical properties of BA, hydrophilic polymers that can enhance the solubility of BA were chosen in order to prepare MQ samples of BA.

Screening and Miscibility of BA/Polymer MQ-SDs

Five structurally diverse hydrophilic polymers were screened for their ability to form amorphous dispersions of BA based on their literature evidence to enhance the solubility of poorly water-soluble NCE (Table I). From Table II, it can be seen that the apparent solubility of BA in the physical mixtures of BA/HPMCAS-HF, BA/Eudragit RLPO,

BA/Kollidon K90, and BA/Kollidon VA64 in 1:4 (*w/w*) ratio in SGF was found to be below the limits of detection by HPLC (<0.2 μg/mL). In comparison, the physical mixture of BA/Soluplus showed an approximately tenfold higher solubility (2.5 μg/mL) in SGF. Almost all the physical mixtures of BA/polymers in 1:4 (*w/w*) ratio showed similar or higher solubility (>twofold for BA/HPMCAS-HF) of BA than neat BA in SIF (Table II), except for BA/Kollidon VA64, which was found to be below the limits of detection by HPLC (<0.2 μg/mL). In order to investigate the effect of intermolecular interactions between BA and the hydrophilic polymers on the solubility and miscibility of BA, MQs of BA/polymer at various ratios and at a fixed drug concentration were prepared and characterized for miscibility and homogeneity.
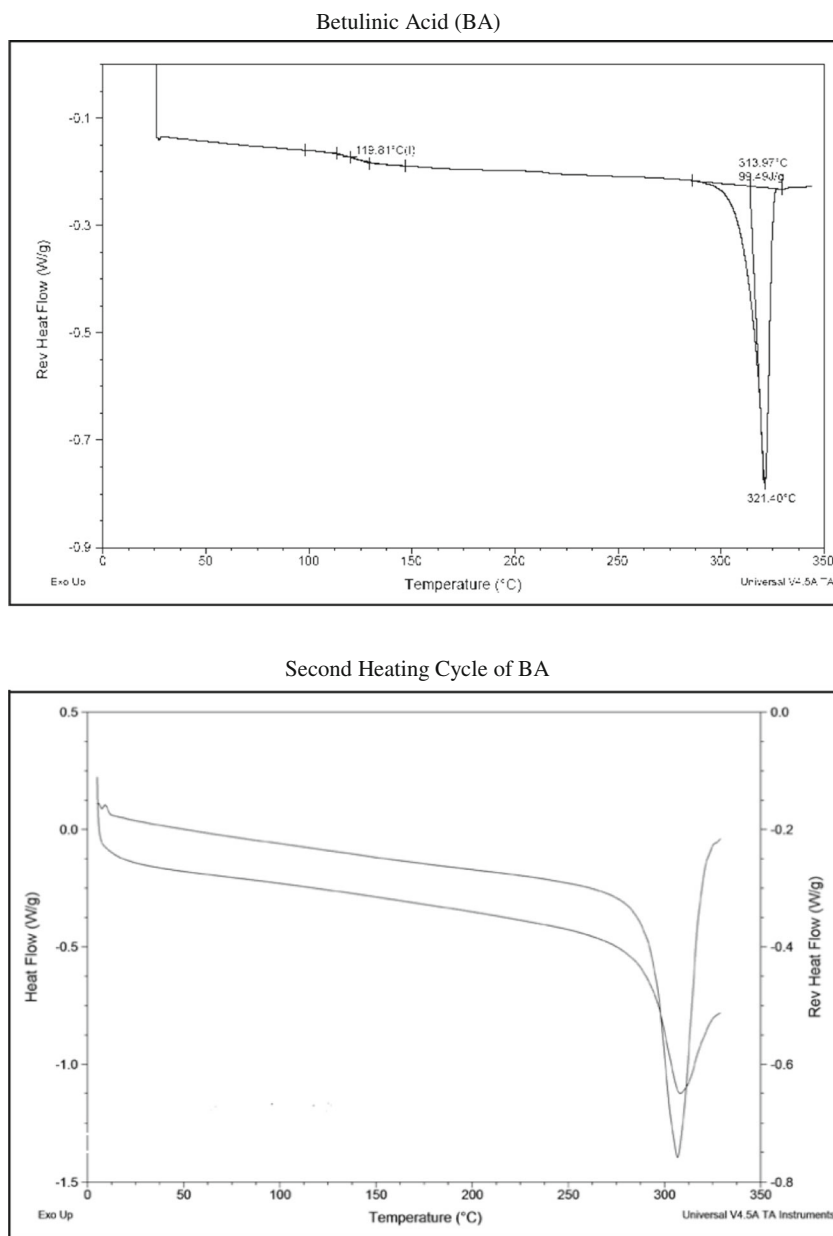

Fig. 2. MDSC profiles of betulinic acid (BA), second heating cycle of BA and BA/polymer melt-quenched solid dispersions (MQ-SDs) at a scanning speed of 10°C/min
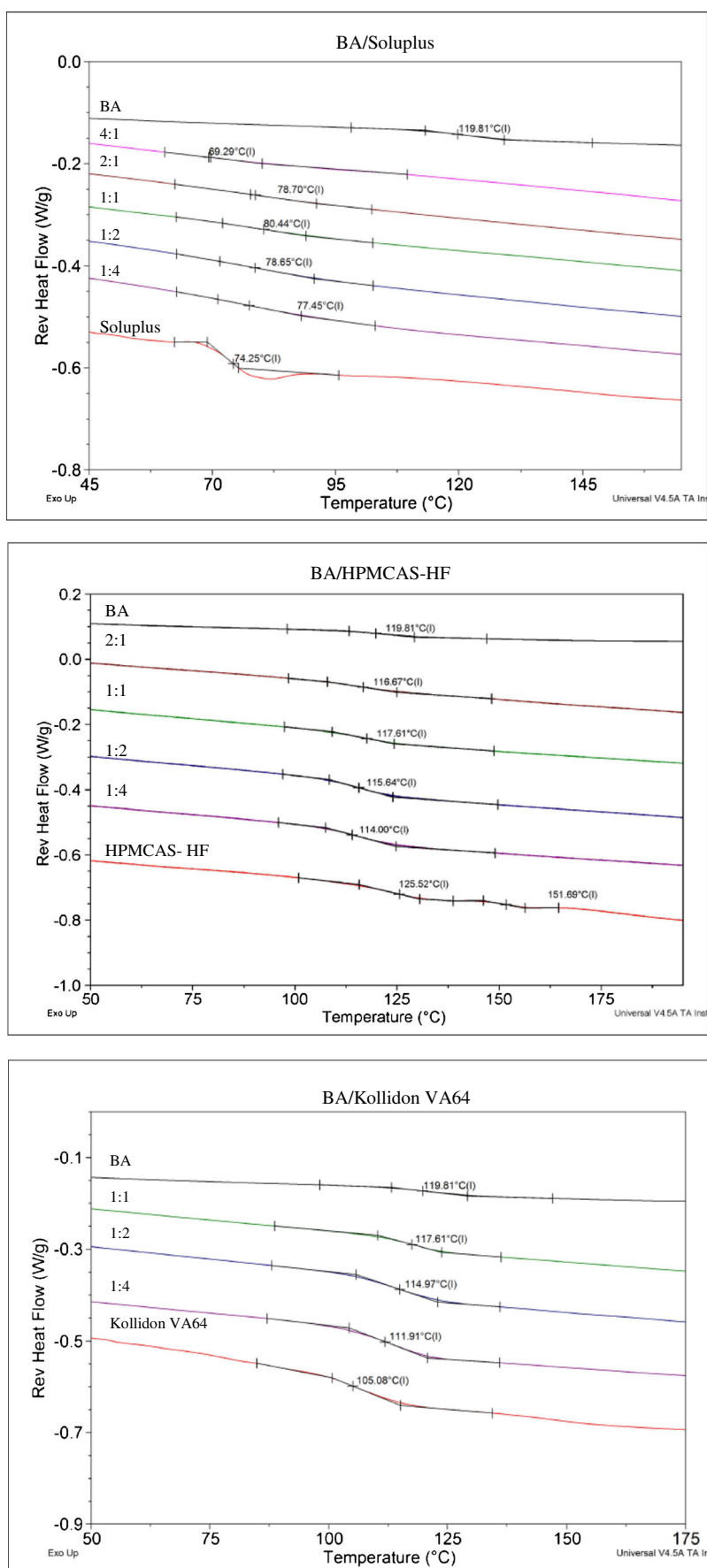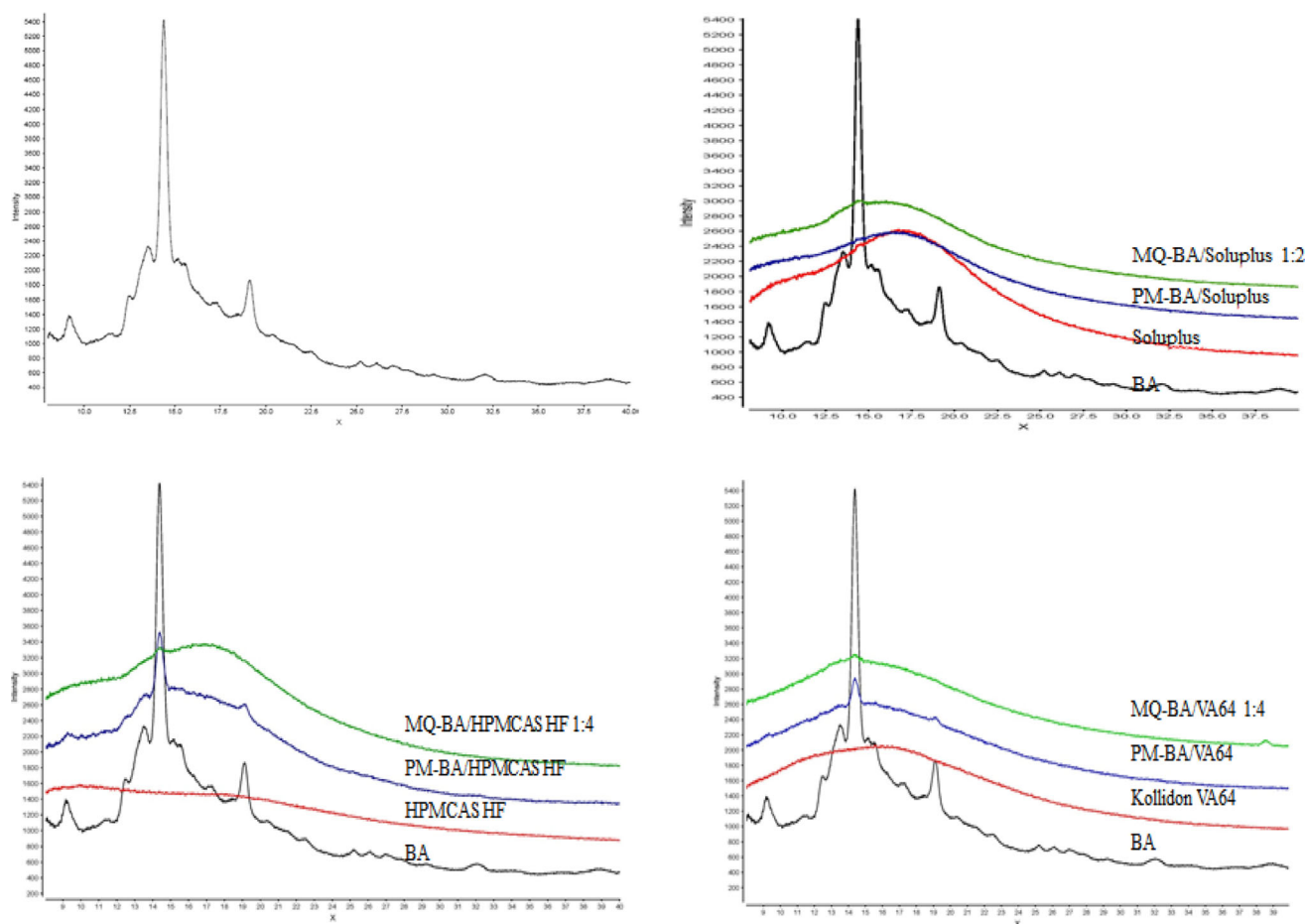
Fig. 2. (continued)

Fig. 3. XRPD patterns of betulinic acid (BA) and BA/polymer MQ-SD at 1:2 or 1:4 *w/w* ratios

The presence of a single *Tg* as detected by the DSC is an indicator of miscibility and a single homogenous phase (42, 43) as the drug-polymer mixture transitions from a liquid or highly viscous solution to supercooled glassy form (42). Therefore, the miscibility and homogeneity of MQ-BA-polymer samples were characterized based on a number of observations of the MDSC profiles.

The MDSC profiles indicated that BA is potentially miscible in all of the polymers at a 1:4 (*w/w*) ratio; their MDSC profiles show the presence of a single *Tg* (~60°C for Eudragit RLPO, ~78°C for Soluplus, ~105°C for Kollidon VA64, ~114°C for HPMCAS-HF, ~178°C for Kollidon K90) and the absence of the drug endotherm at a higher drug loading concentration (Fig. 2). Moreover, chemical degradation studies indicated that approximately 100–105% of BA was recovered from the MQ-SDs of BA with Soluplus, HPMCAS-HF, Kollidon VA64, and Kollidon K90 whereas 95% of BA was recovered from BA/Eudragit RLPO MQ-SD (Table III). As the concentration of BA increased in the blends, the melting endotherm for the drug was apparent only for Kollidon K90 (Supporting Data Fig. S1) and can be related to the concentration of the polymer in the mixture. The reverse was the case for the polymers, where the *Tg* of the polymer was less apparent at higher drug loading for Soluplus, HPMCAS-HF, and Kollidon VA64. The miscibility of BA in the hydrophilic polymers was further substantiated by the solubility studies. As evident from Table II, the MQ-SD with Soluplus exhibited the highest solubility of BA (32.8 μg/mL in SGF and 30.5 μg/mL in

SIF) than any other hydrophilic polymers (MQ-SDs of HPMCAS-HF, Eudragit RLPO, Kollidon VA64, and Kollidon K90 in SIF have solubilities in the range of 1–4 μg/mL) and compared to that of neat BA in SIF (1.8 μg/mL). The solubility of BA in MQ-SD with Soluplus was approximately 15-fold higher in SGF and SIF compared to the solubility of neat BA in SGF and SIF. In addition, the MQ-SD of Kollidon VA 64 also exhibited a significant improvement in solubility in SIF (4 μg/mL) compared to the solubility of its PMs in both SGF and SIF (<0.2 μg/mL).

Apart from the chemical structure of the polymer, the concentration of the polymer can be a critical contributor to the stabilization of the amorphous MQ-SD. Several methods (Gordon-Taylor and Fox equation) can be used to model the dependence of the polymer concentration on the *Tg* of the drug-polymer mixture. In this study, we applied the Fox equation (44) to predict the *Tg* of the drug-polymer mixture, which is based on the sum of the weight fractions of each component in the mixture and is given by

$$1/Tg = w1/Tg1 + w2/Tg2$$

where *Tg* is the glass transition temperature of the blend, *Tg*1 and *Tg*2 are the glass transition temperatures of pure components 1 and 2, respectively, and w1 and w2 are the weight fractions of components 1 and 2, respectively. It follows that if

(i)

(ii)

(iii)

(iv)

(v)

(vi)

(vii)

(viii)
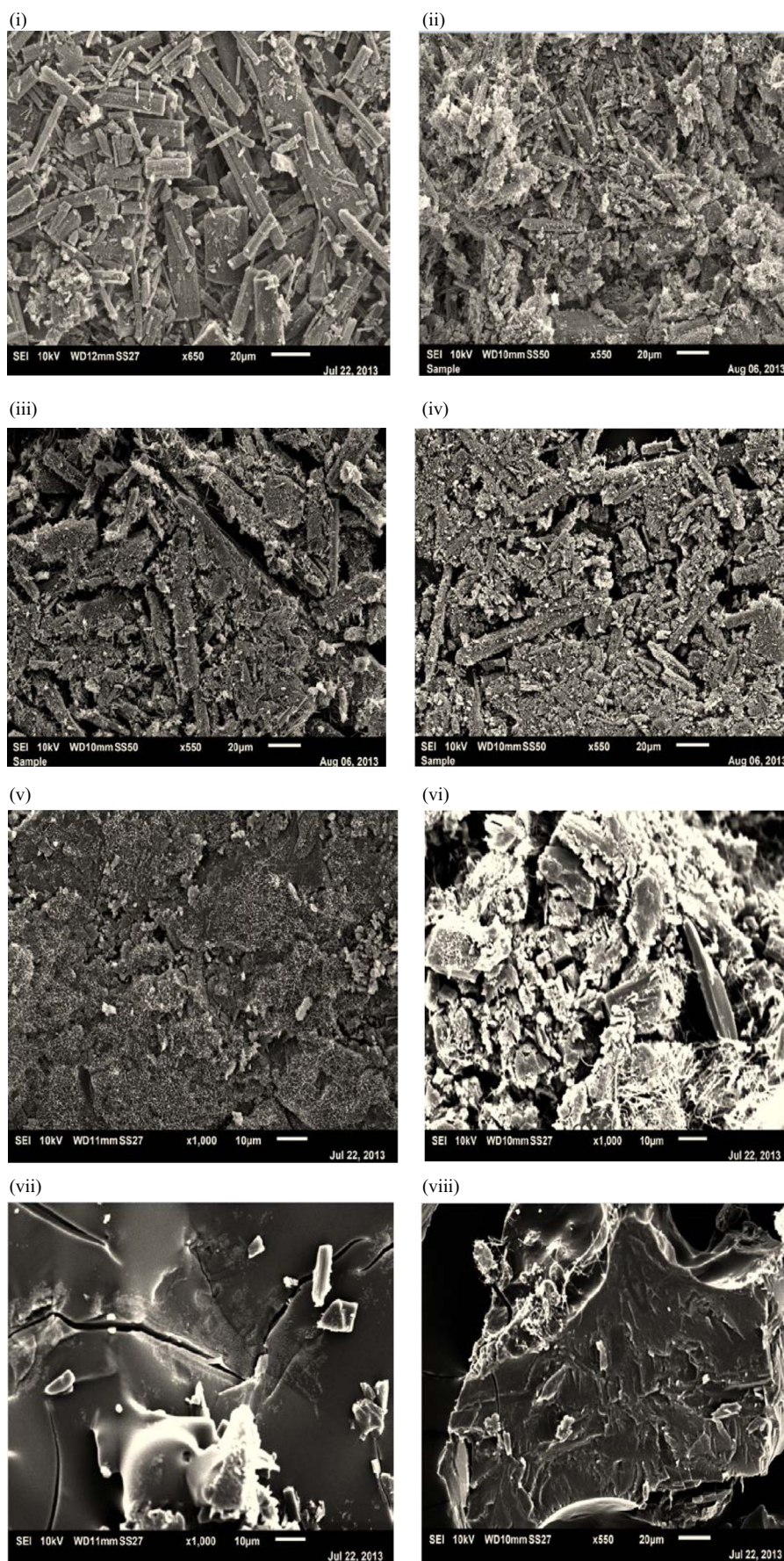
Fig. 4. SEM images of betulinic acid (BA) and BA/polymer MQ-SD at 1:2 or 1:4 *w/w* ratios
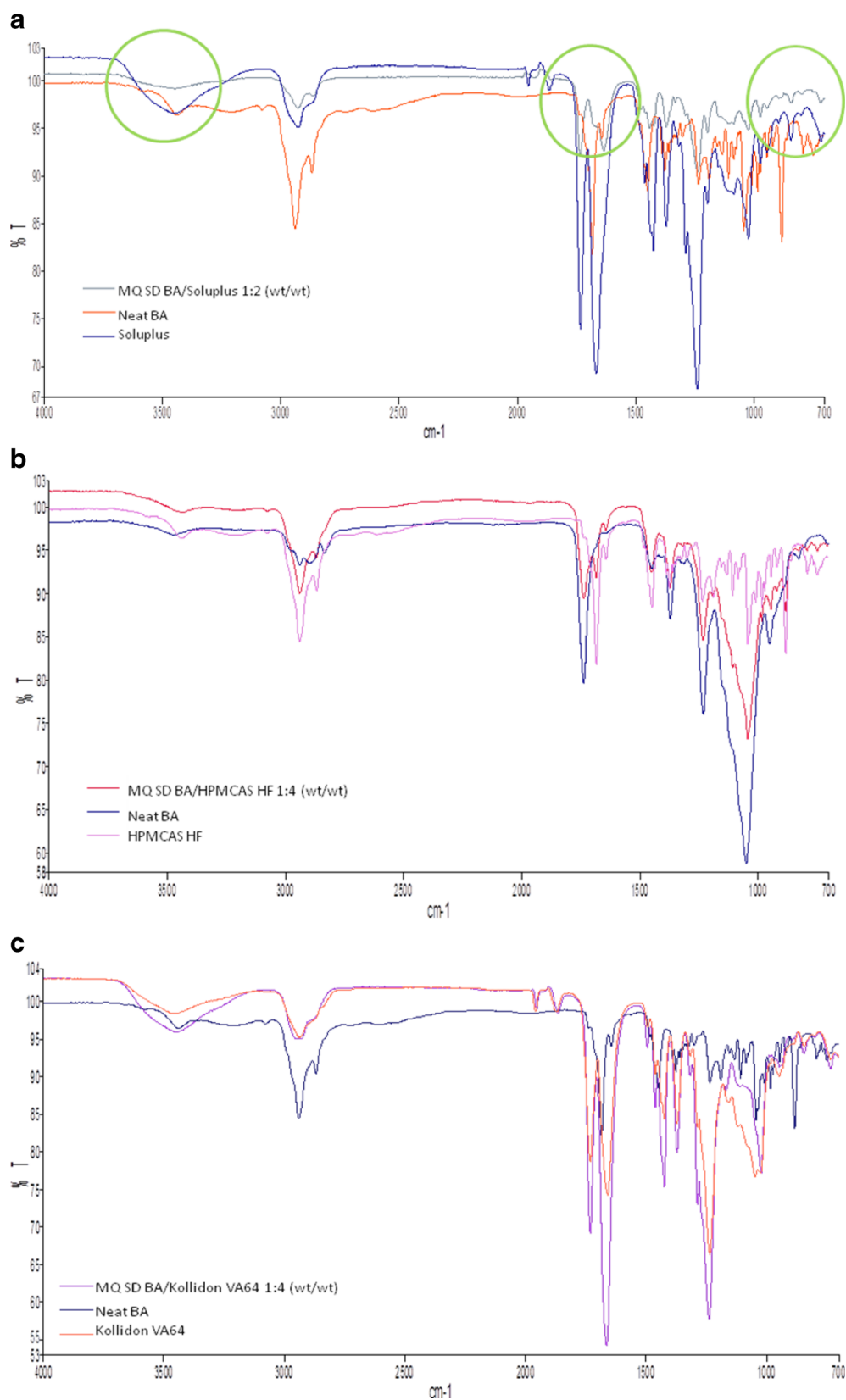
Fig. 5. FT-IR spectrum of betulinic acid (BA) and BA/polymer MQ-SD at 1:2 or 1:4 *w/w* ratios

the two components are miscible, the experimentally obtained *Tg* values should follow the shape of the predicted curves. The use of Fox equation requires the measurement of *Tg* of neat

BA which was found to be ~119.8°C in our study. The predicted *Tg* values of the blends are presented in Fig. 6. The experimentally measured *Tg* values of MQ-SD of BA

Table II. Solubility of BA/Polymer Physical Mixture (PM) and Melt-Quenched Solid Dispersion (MQ-SD) in Simulated Gastric Fluid (SGF) and Simulated Intestinal Fluid (SIF)

	Solubility[a] (µg/mL)			
	PM		MQ-SD	
BA/polymers	SGF	SIF	SGF	SIF
Neat betulinic acid (BA)	0.0	1.8±0.4	0.0	0.0
BA/Soluplus	2.5±0.5	2.3±1.1	33±1.2	31±0.3
BA/HPMCAS-HF	0.0	4.5±2.8	0.0	0.8±0.0
BA/Eudragit RLPO	0.0	1.4±0.4	0.0	0.7±1.2
BA/Kollidon VA 64	0.0	0.0	0.0	3.8±0.2
BA/Kollidon K90	0.0	2.2±1.2	0.1±0.2	0.3±0.6

[a] Data are represented as the means ± SD

with Eudragit RLPO (Fig. 6c) and Kollidon K90 (Supporting Data Fig. S2) indicated almost no correlation with the predicted Tg values at all concentrations of BA, and the slopes of the experimental curves were almost flat, which suggests that miscible systems were not achieved. On the other hand, experimentally obtained Tg of MQ-SD with Eudragit RLPO and PVP K90 shows a constant slope from the predicted value. These results were substantiated by the low solubility of BA in the MQ-SDs with Eudragit RLPO and Kollidon K90 in SIF (Table II).

In the case of Soluplus and HPMCAS-HF (Fig. 6a and b, respectively), few experimentally obtained Tg values closely matched the predicted value, and clearly, exponential curves were observed, which suggests partial miscibility of BA (1:4–1:1 (w/w) ratio of BA/Soluplus and 1:1 (w/w) ratio of BA/HPMCAS-HF) with the polymers. Among the polymers under investigation in this study, the experimental values obtained for MQ-SDs with Kollidon VA64 (Fig. 6d) produced experimental Tg values that correlated well with the predicted one, which implied that potential miscibility of BA may have been achieved at all drug-polymer ratios. These results were supported by the solubility studies of BA where the MQ-SD with Soluplus was found to have the highest apparent solubility in SIF (30.5 µg/mL) followed by Kollidon VA64 (3.8 µg/mL). Since, few experimentally obtained Tg values matched the predicted value for Soluplus, we would have expected the solubility of BA in MQ-SD with Soluplus to be lower than that with Kollidon VA-64, which was clearly not the case. The MQ-SD of HPMCAS-HF had lower solubility in SIF than the physical mixture of BA/HPMCAS-HF.

Solid-State Characterization of BA/Polymer MQ-SDs

Because there is no single analytical technique that can unambiguously predict the miscibility and homogeneity of the MQ-SDs of BA with the polymers, therefore a number of analytical tools including XRPD, SEM, and FT-IR were utilized to elucidate the solid-state characteristics of the MQ-SDs of BA dispersed within the polymer matrix. Scanning electron micrographs, XRPD patterns, and FT-IR spectra of BA/polymer MQ-SDs at ratios that indicate the potential incorporation of BA in the SD systems are shown in Figs. 3, 4, and 5, respectively. The XRPD which is a non-invasive technique indicated that BA/Soluplus (1:2 w/w), BA/HPMCAS-HF (1:4 w/w), and Kollidon VA64 (1:4 w/w) MQ-SDs are amorphous due to the absence of crystalline peaks of BA (Fig. 3) as compared to the physical mixture. The SEM images of BA/Soluplus and BA/HPMCAS-HF MQ-SDs appear to be spongy and porous with the particles in the sub-micron range (10 µm). There is no evidence of crystalline BA in the SEM images of BA/Soluplus and BA/HPMCAS-HF MQ-SDs as either separate crystals or spread within the MQ-SD as seen in Fig. 4b (v–vi). From these results, it can be concluded that BA is probably uniformly dispersed within the polymer matrix in the MQ-SDs of Soluplus, HPMCAS-HF, and Kollidon VA64 and can stabilize the amorphous drug for an extended time period.

Solid dispersions are well documented to form spontaneously through strong interactions (e.g., ionic and hydrogen bond interactions) if the components are miscible (45), as observed with BA, Soluplus, and HPMCAS-HF. Moreover, if BA interacts with a polymer in a solid dispersion, the

Table III. Degradation Profile of BA/Polymer Melt-Quenched Solid Dispersion (MQ-SD)

BA/polymers	BA recovery[a] (%)	Total degradation (%)
Pre-MQ neat betulinic acid (BA)	100.4±0.026	0.51
MQ-neat BA	105.1±0.002	0.63
BA/Soluplus	102.7±0.007	1.16
BA/HPMCAS-HF	102.95±0.015	1.17
BA/Eudragit RLPO	94.87±0.022	2.12
BA/Kollidon VA 64	100.66±0.026	2.79
BA/Kollidon K90	103.66±0.019	0.82

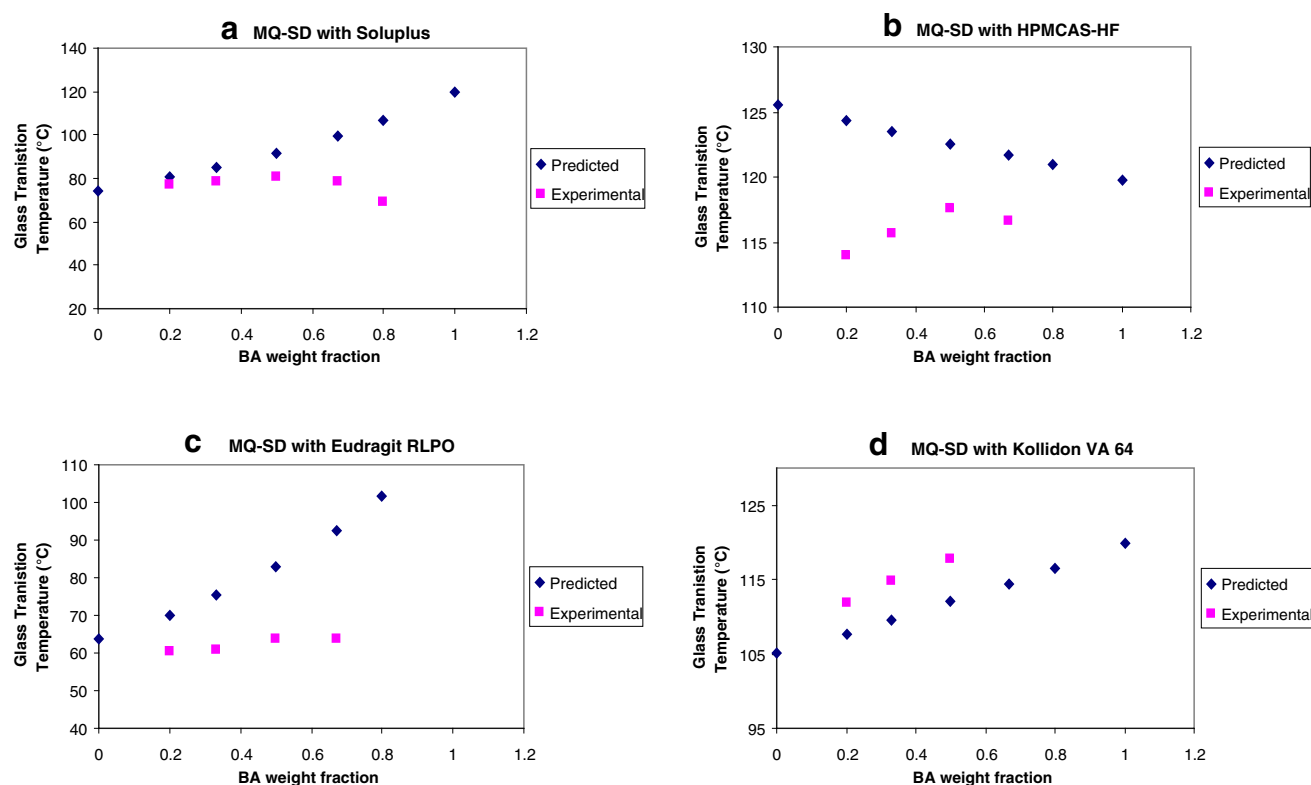[a] Data for BA recovery are represented as the means ± SD

Fig. 6. Comparison of predicted glass transition temperatures (*Tg*) of BA/polymer melt-quenched solid dispersions (MQ-SDs) by the Fox equation and experimental values

functional groups in the FT-IR spectra of the solid dispersion would show band shifts and broadening compared to the spectra of the pure drug and polymers (46). Among the FT-IR spectra of BA/Soluplus, BA/HPMCAS-HF, and BA/Kollidon VA64 MQ-SDs, the spectrum of the BA/Soluplus MQ-SD showed substantial differences in the 3,200–3,600 cm^{-1}, 1,700–1,500 cm^{-1}, and 1,000–700 cm^{-1} regions. The differences observed between the FT-IR spectrum of the BA/Soluplus MQ-SD and that of BA are shown in Fig. 5a and includes (1) broadening of the O–H stretching band due to the −OH group at C-3 position in BA between 3,600 and 3,200 cm^{-1}; (2) shifting of the C=O stretching bands at 1,684 and 1,667 cm^{-1} in the spectra of pure BA and Soluplus, respectively; and (3) the appearance of two strong bands in the spectrum of the BA/Soluplus MQ-SD at 1,733 cm^{-1} due to the shift in the C=O stretching bands at 1,667 cm^{-1} in Soluplus and 1,237 cm^{-1} which is due to the contributions from the C–H stretching in Soluplus. Vibrational changes in the O–H stretching band in the spectrum of BA and the −C=O stretching of the carbonyl group in the spectrum of Soluplus suggest the formation of a hydrogen bond between the carbonyl group in Soluplus and the hydroxyl group at C-3 position in BA. Although the −C=O and N–H functionalities in Soluplus, Kollidon VA64, and Kollidon K90 can hydrogen bond with the O–H group at C-3 position in BA, the −C=O group is sterically more accessible than N–H to form hydrogen bond with the O–H group at C-3 position in BA. The FT-IR spectra for BA/HPMCAS-HF and BA/Kollidon VA64 did not show any noticeable broadening of the O–H stretching band between 3,600 and 3,200 cm^{-1} nor could any shifting of the

−C=O stretching bands at 1,684 cm^{-1} be observed, indicating weak intermolecular interactions between BA/HPMCAS-HF and BA/Kollidon VA64, which was reflected by the low solubility of the MQ-SDs with these polymers in SIF (Table II). On the other hand, there is clear evidence for crystalline peaks of BA for BA/Eudragit RLPO (1:4 *w/w*) and BA/PVP K90 (1:4 *w/w*) MQ-SDs in the XRPD, suggesting that as the *Tg* of the BA/Eudragit RLPO (1:4 *w/w*) and BA/PVP K90 (1:4 *w/w*) system was depressed, the samples were converted to a supercooled liquid, which caused increased molecular mobility in the BA/Eudragit RLPO (1:4 *w/w*) and BA/PVP K90 (1:4 *w/w*) MQ-SD system and lead to the recrystallization of BA. The conversion of the BA/Eudragit RLPO (1:4 *w/w*) and BA/PVP K90 (1:4 *w/w*) system to a supercooled liquid is reflected in the SEM images (Fig. 4 (vii–viii)) by the presence of a smooth glassy surface and crystalline drug material, indicating a possible phase separation. No significant changes in the molecular vibrations were observed from the FT-IR spectra of the BA/Eudragit RLPO and BA/PVP K90 MQ-SDs too (Supporting Data Fig. S5). These results correlate well with the findings of predicted and experimental *Tg* values using the Fox equation (Fig. 6) that these polymers probably would not form miscible systems and stabilize the amorphous drug and by the low solubility of the MQ-SDs with these polymers in SIF (Table II).

Chemical Characterization of BA/Polymer MQ-SDs

In order to further evaluate the selection of potential polymers for the fabrication of BA solid dispersions, the

concentration of BA in the MQ-SDs, the degradation profiles of the BA/Soluplus and BA/Kollidon K90 MQ-SDs prepared at a ratio of 1:2 (*w/w*), and the degradation profiles of the BA/HPMCAS-HF, BA/Eudragit RLPO, and BA/Kollidon VA64 MQ-SDs prepared at a ratio of 1:4 (*w/w*) were evaluated by HPLC. The concentration of BA in neat BA subjected to the melt-quench treatment was used as a control. Recoveries of BA from the MQ-SDs of BA with Soluplus, HPMCAS-HF, Kollidon VA64, and Kollidon K90 fell in the range of 98–104%, whereas that from BA/Eudragit RLPO MQ-SD was 88%. The BA MQ-SD with HPMCAS-HF showed the least amount of degradation (1.2%). The percent degradation of the BA/Soluplus and the BA/Kollidon K90 MQ-SDs was comparable to that of the control (1.17 and 0.82%, respectively), whereas the BA/Eudragit RLPO and the BA/Kollidon VA64 MQ-SDs exhibited the highest amount of degradation among all the samples, as shown in Table III.

DISCUSSION

Betulinic acid, a novel natural product obtained from the outer bark of many trees including birch trees, has shown tremendous promise in clinical trials as an antimelanoma and anti-HIV agent. The development of BA has been hampered by its poor aqueous solubility. The objective of this study was to determine the feasibility of fabricating solid dispersions of BA and hydrophilic polymers with the aim of enhancing the apparent solubility of BA. In order to test our hypothesis, in this part I study, we compared the miscibility, the molecular structures, the solid state, the chemical state, and the performance of solid dispersions of BA in different polymers in terms of their solubility to identify the most ideal polymer for producing a stable solid dispersion of BA. In order to prepare solid dispersion of BA with the polymers, the melt-quench (MQ) method was adopted for this study. The solubility of neat BA in simulated gastric fluid (SGF) was found to be below the limits of detection by HPLC which was not unexpected as BA is a weak acid with a pKa of 4.6. Weak acids are more soluble at higher pH which was the case (1.8 μg/mL in SIF) when neat BA was dissolved in simulated intestinal fluid (SIF). Based on the physico-chemical properties of BA, the feasibility of forming amorphous solid dispersion of BA in order to enhance the apparent solubility of the drug will depend on the chemical structure of the polymer and its ability to form intermolecular interactions (i.e., hydrogen bonds or weaker interactions) with −OH group at C-3 position and/or an ionizable −COOH group at C-28 position in BA and stabilize amorphous BA from conversion to the crystalline form as substitutions at these positions in BA have been shown to greatly enhance the solubility and efficacy of BA analogs. If the drug and polymer are only partially miscible in each other or if the drug is not molecularly dispersed in the polymer matrix, crystalline drug molecules in the polymer matrix can serve as a nucleus for crystallization. In this case, a third component would have to be introduced to ameliorate the conversion. Even if full miscibility of the two components can be achieved, the conversion of the amorphous form of the drug to its crystalline form can occur because the system is at a high-energy state, and the molecules will tend to rearrange and phase-separate during storage.

The miscibility and homogeneity of MQ-BA-polymer samples were characterized based on a number of observations of the MDSC profiles. The *Tg* of the drug was compared with respect to the polymer to observe for the presence of a single homogeneous phase as the drug-polymer mixture transitions from a liquid or highly viscous solution to a supercooled glassy form (42,43). A single *Tg* is an indicator of a single drug-polymer phase, whereas the presence of more than one *Tg* can indicate immiscibility or phase separation of the drug-polymer mixture. The melting point depression of BA was examined which may change due to the miscibility of the drug in the polymer as a consequence of heating. In addition, we observed for the presence of amorphous drug in the MQ samples by monitoring the drug *Tg* and the appearance of recrystallization exotherm in the MDSC profile. All five of the investigated polymers (Soluplus, HPMCAS-HF, Eudragit RLPO, Kollidon VA64, and Kollidon K90) were found to be miscible with BA as indicated by MDSC analysis, although the ratio of the polymer that can completely incorporate BA in the system varies. This variation suggests that BA can be molecularly dispersed in the polymers only up to a certain compositional range. By increasing the concentration of the polymer in the mixture up to a certain concentration range, the amount of energy that is available to break the crystal lattice increases, suggesting the immobilization of the drug in the polymer matrix. Soluplus, HPMCAS-HF, and Kollidon VA64 were found to be the most feasible solid dispersion carriers for BA indicating that the polymers are able to provide sufficiently high *Tg* values to the MQ-SDs that can stabilize the amorphous MQ-SDs. There are many examples in the literature where polymers such as HPMCAS and Soluplus have been shown to provide stability to the amorphous drugs like vemurafenib and griseofulvin through hydrogen bond formation. (47,48). A closer examination of the chemical structure of Soluplus indicates that the carbonyl group of the vinylcaprolactam and/or vinylacetate lipophilic side chain has the ability to hydrogen bond with the hydroxyl group at the C-3 position in BA which can stabilize the amorphous form of BA for an extended period. On the other hand, polymers that have the propensity to coalesce and form dimers or heterodimers usually exhibit lower *Tg* values when molecularly mixed with the drug. In such cases, the difference between the experimentally obtained *Tg* and predicted value will be great due to the drug-polymer and drug-drug interactions. This is probably due to the fact that Eudragit RLPO and Kollidon K90 has been shown to coalesce due to the presence of plasticizing and non-plasticizing water trapped within the polymeric structure (49) and therefore probably have minimal molecular interactions with the drug. In cases where the drug demonstrates strong intermolecular interactions with the polymer such as Soluplus, the *Tg* will be higher as the binding of the drug to the polymer retards molecular mobility or β-relaxations of the polymer chain. Since β-relaxations usually occur at lower *Tg* (*Tg*-50°C) and are precursors to the α-relaxations, the molecular mobility of the entire molecule can be affected. The ability of Soluplus, HPMCAS-HF, and Kollidon VA64 to provide higher *Tg* to the BA-polymer mixture could stabilize the amorphous drug and improve the solubility of the poorly water-soluble drug. On the other hand, there is clear evidence

for crystalline peaks of BA for BA/Eudragit RLPO (1:4 *w/w*) and BA/PVP K90 (1:4 *w/w*) MQ-SDs in the XRPD, which was evident from the MDSC profile. As the *Tg* of the BA/Eudragit RLPO (1:4 *w/w*) and BA/PVP K90 (1:4 w/w) system was depressed, the samples were converted to a supercooled liquid which caused increased molecular mobility in the BA/Eudragit RLPO (1:4 *w/w*) and BA/PVP K90 (1:4 w/w) MQ-SD system and lead to the recrystallization of BA.

Evaluation of the solubilities of the BA/polymer MQ-SDs in SGF and SIF indicated that the MQ-SD of Soluplus exhibited a remarkable improvement in solubility in SGF and in SIF compared to the MQ-SDs of HPMCAS-HF and Kollidon VA64. The formation of a hydrogen bond between the −C=O group in Soluplus and O–H at C-3 position in BA, which was indicated by the FT-IR spectra, would cause a significant improvement in the apparent solubility of BA as reported by the vast number of BA analogs synthesized—notable among them is Bevirimat (i.e., PA-457 or 3-*O*-(3′,3′-dimethylsuccinyl)) derivative of BA (11), the HIV-1 maturation inhibitor. A possible explanation for the lower solubility of MQ-SD of HPMCAS-HF in simulated biofluids as compared to Soluplus could be due to the fact that HPMCAS-HF probably hydrolyzed to release free succinic acid under the experimental conditions which retarded the aqueous solubility of BA (50). In contrast to HPMCAS-HF, PVP VA64 (γ-butyrolactam), PVP K90 (γ-butyrolactam), and Soluplus (ε-caprolactam) are all lactam-containing polymers. Soluplus has been shown to increase the solubilization of poorly water-soluble drugs irrespective of their structure by forming micelles of drug complex with the vinylcaprolactam and vinylacetate lipophilic side chains as compared to PVP VA64 and PVP K90. In addition, since BA is a pentacyclic triterpenoid, it assumes a *trans*-decalin conformation such that the hydroxyl group at C-3 position in BA can form a hydrogen bond with the carbonyl groups in vinylcaprolactam and/or vinylacetate more readily with Soluplus as compared to Kollidon VA64 or any other polymer, which would explain the difference in the solubility of BA when complexed with different polymers. The MQ-SD of BA/Eudragit RLPO (1:2, *w/w*) with a *Tg* of ~61.0°C may lead to stability issues because stable amorphous systems require a *Tg* of at least 50°C higher than the storage temperature. Therefore, if these systems are to be used for formulation development, the storage temperatures would have to be <11°C on the basis of a rough approximation. In addition to the reduced *Tg*, solid-state and chemical-state characterization showed a disadvantage of the BA/Eudragit system, as indicated by the presence of crystalline peaks attributable to BA in the XRPD pattern of the MQ-SD of BA/Eudragit RLPO system and the lowest assay values and highest degradation of BA. In the case of Kollidon K90, an amorphous solid dispersion was not formed, which is consistent with the lack of correlation between the predicted and experimental *Tg* values and could be due to the fact that no hydrogen bond interactions were observed between Kollidon K90 and BA in the FT-IR spectra.

CONCLUSION

Based on the cumulative analytical data obtained in this study, there is little possibility for MQ-SD of BA/Soluplus,

HPMCAS-HF, and Kollidon VA64 at 1:4 (*w/w*) ratio to cause stability issues and recrystallize to crystalline BA due to the high *Tg* value of the MQ-SD, amorphous nature of the MQ-SD, and molecular interactions with the excipients. In order to confirm our hypothesis, studies are in progress to determine the long-term stability and the dissolution kinetics of the MQ-SD of BA/Soluplus, HPMCAS-HF, and Kollidon VA64 the data for which will be included as a follow-up to this part I study.

In conclusion, the rank order of polymers suitable for the formulation of BA solid dispersions as a binary system is Soluplus > Kollidon VA64 > HPMCAS-HF. In general, the carrier that can molecularly interact with BA to enhance the apparent solubility and stability of BA will be the most favorable option; however, the desired pharmacokinetics profile, desired dose, target delivery site, and stability of the formulation will also have to be taken into consideration.

REFERENCES

1. Kim J, Park EJ. Cytotoxic anticancer candidates from natural resources. Curr Med Chem Anticancer Agents. 2002;2:485–537.
2. Kessler JH, Mullauer FB, de Roo GM, Medema JP. Broad invitro efficacy of plant-derived betulinic acid against cell lines derived from the most prevalent human cancer types. Cancer Lett. 2006;251:132–45.
3. Kim JY, Koo HM, Kim DS. Development of C-20-modified betulinic acid derivatives as antitumor agents. Bioorg Med Chem Lett. 2001;11:2405–8.
4. Mullauer FB, Kessler JH, Medema JP. Betulinic acid, a natural compound with potent anticancer effects. Anticancer Drugs. 2010;21(3):215–27.
5. Mullauer FB, van Bloois L, Daalhuisen JB, Ten Brink MS, Storm G, Medema JP, *et al*. Betulinic acid delivered in liposomes reduces growth of human lung and colon cancers in mice without causing systemic toxicity. Anticancer Drugs. 2011;22(3):223–33.
6. Zuco V, Supino R, Righetti SC, Cleris L, Marchesi E, Gambacorti-Passerini C. Selective cytotoxicity of betulinic acid on tumor cell lines, but not on normal cells. Cancer Lett. 2002;175:17–25.
7. Fulda S, Kroemer G. Targeting mitochondrial apoptosis by betulinic acid in human cancers. Drug Discov Today. 2009;14:885–90.
8. Fulda S, Scaffidi C, Susin SA, Krammer PH, Kroemer G, Peter ME. Activation of mitochondria and release of mitochondrial apoptogenic factors by betulinic acid. J Biol Chem. 1998;273:33942–8.
9. Clinical Trials "Evaluation of 20% betulinic acid ointment for treatment of dysplastic nevi (moderate to severe dysplasia)" http://clinicaltrials.gov/show/NCT00346502.
10. De Clercq E. Highlights in the development of new antiviral agents. Mini Rev Med Chem. 2002;2(2):163–75.
11. Hashimoto F, Kashiwada Y, Cosentino LM, Chen C, Garrett PE, Lee KH. Anti-AIDS agents-XXVII. Synthesis and anti-HIV activity of betulinic acid and dihydrobetulinic acid derivatives. Bioorg Med Chem. 1997;12:2133–43.
12. Jäger S, Winkler K, Pfüller U, Scheffler A. Solubility studies of oleanolic acid and betulinic acid in aqueous solutions and plant extracts of Viscum album L. Planta Med. 2007;73(2):157–62.

13. Claude B, Morin P, Lafosse M, Andre P. Evaluation of apparent formation constants of pentacyclic triterpene acids complexes with derivatized β- and γ-cyclodextrins by reversed phase liquid chromatography. J Chromatogr A. 2004;1049(1–2):37–42.

14. Dehelean CA, Soica C, Peev C, Ciurlea S, Feflea S, Kasa P. A pharmaco-toxicological evaluation of betulinic acid mixed with hydroxipropilgamma cyclodextrin on in vitro and in vivo models. Farmacia. 2011;59(1):51–9.

15. Soica CM, Dehelean CA, Peev CI, Coneac G, Gruia AT. Complexation with hydroxypropyl-γcyclodextrin of some pentacyclic triterpenes. Characterisation of their binary products. Farmacia. 2008;56(2):182–90.

16. Ciurlea SA, Dehelean CA, Ionescu D, Berko S, Csanyi E, Hadaruga DI, et al. A comparative study regarding melanoma activity of betulinic acid on topical ointment vs. systemic nanoemulsion delivery systems. J Agroaliment Process Technol. 2010;16(4):420–6.

17. Dehelean CA, Feflea S, Ganta S, Amiji M. Anti-angiogenic effects of betulinic acid administered in nanoemulsion formulation using chorioallantoic membrane assay. J Biomed Nanotechnol. 2011;7(2):317–24.

18. Sharma G, Anabousi S, Ehrhardt C, Ravi Kumar MN. Liposomes as targeted drug delivery systems in the treatment of breast cancer. J Drug Target. 2006;14:301–10.

19. Janssens S, Van den Mooter G. Review: physical chemistry of solid dispersions. J Pharm Pharmacol. 2009;2009(12):1571–86.

20. Leuner C, Dressman J. Improving drug solubility for oral delivery using solid dispersions. Eur J Pharm Biopharm. 2000;50:47–60.

21. Sun Y, Tao J, Zhang GGZ, Yu L. Solubilities of crystalline drugs in polymers: An improved analytical method and comparison of solubilities of indomethacin and nifedipine in PVP, PVP/VA, and PVAc. J Pharm Sci. 2010;99(9):4023–31.

22. Chiou W, Reigelman S. Pharmaceutical applications of solid dispersion systems. J Pharm Sci. 1971;60:1281–302.

23. Qian F, Huang J, Zhu Q, Haddadin R, Gawel J, Garmise R, et al. Is a distinctive single Tg a reliable indicator for the homogeneity of amorphous solid dispersion? Int J Pharm. 2010;395:232–5.

24. Rumondor ACF, Ivanisevic I, Bates S, Alonzo DE, Taylor LS. Evaluation of drug-polymer miscibility in amorphous solid dispersion systems. Pharm Res. 2009;26(11):2523–34.

25. Hancock BC, Zografi G. Characteristics and significance of the amorphous state in pharmaceutical systems. J Pharm Sci. 1997;86(1):1–12.

26. Le-Ngoc Vo C, Park C, Lee B-J. Current trends and future perpectives of solid dispersions containing poorly water-soluble drugs. Eur J Pharm Biopharm. 2013;85:799–813.

27. Andronis V, Zografi G. Molecular mobility of supercooled amorphous indomethacin determined by dynamic mechanical analysis. Pharm Res. 1997;14(4):410–4.

28. Hancock BC, Shamblin S, Zografi G. Molecular mobility of amorphous pharmaceutical solids below their glass transition temperatures. Pharm Res. 1995;12:799–806.

29. Bhattacharya S, Suryanarayanan R. Local mobility in amorphous pharmaceuticals—characterization and implications on stability. J Pharm Sci. 2009;98(9):2935–53.

30. Fekete E, Foldes E, Pukanszky B. Effect of molecular interactions on the miscibility and structure of polymer blends. Eur Poly J. 2005;41:727–36.

31. Bley H, Fussnegger B, Bodmeier R. Characterization and stability of solid dispersions based on PEG/polymer blends. Int J Pharm. 2010;390(2):165–73.

32. Forster A, Hempenstall J, Tucker I, Rades T. Selection of exciepients for melt extrusion with poorly water-soluble drugs by solubility parameter calculation and thermal analysis. Int J Pharm. 2001;226:147–61.

33. Löbmann K, Laitinen R, Strachan C, Rades T, Grohganz H. Aminoacids as co-amorphous stabilizers for poorly water-soluble drugs-Part 2: Molecular interactions. Eur J Pharm Biopharm. 2013;85:882–8.

34. BASF technical information, Kollidon®VA64 Kollidon®VA64 Fine, August 2011.

35. Hardung H, Djuric D, Ali S. Combining HME & solubilization: Soluplus®—the solid solution. Drug Del. Tech. 2010; 10(3).

36. Van Den Mooter G. The use of amorphous solid dispersions: a formulation strategy to overcome poor solubility and dissolution rate. Drug Discov Today: Technol. 2012; e79-85.

37. Tanno F, Nishiyama Y, Kokubo H, Obara S. Evaluation of hydromellose acetate succinate (HPMCAS) as a carrier in solid dispersions. Drug Dev Ind Pharm. 1999;30:9–17.

38. Bühler V. Kollidon® Polyvinylpyrrolidone for the pharmaceutical industry, BASF technical infomation, 4th Edition, 1998.

39. Curatolo W, Nightingale JA, Herbig SM. Utility of hydroxypropylmethylcellulose acetate succinate (HPMCAS-HF) for initiation and maintenance of drug supersaturation in the GL milieu. Pharm Res. 2009;26(6):1419–31.

40. Folttmann H, Quadir A. Polyvinylpyrrolidone (PVP)—one of the most widely used excipients in pharmaceuticals: an overview. Drug Del Technol. 2008;8(6):22–7.

41. Hoti E, Qendro G, Censi R, Martino RD, Malaj L. Investigation of the drug stability at the amorphous state using thermal analysis. J. Chem. Chem. Eng. 2012; (6): 646-650.

42. Newman A, Knipp G, Zografi G. Assessing the performance of amorphous solid dispersions. J Pharm Sci. 2012;101(4):1355–77.

43. Shamblin SL, Tang X, Chang L, Hancock BC, Pikal MJ. Characterization of the time scales of molecular motion in pharmaceutically important glasses. J Phys Chem B. 1999;103:4113–21.

44. Brostow W, Chiu R, Kalogeras IM, Vassilikou-Dova A. Prediction of glass transition temperatures: binary blends and copolymers. Mat Let. 2008;62:3152–5.

45. Gryezke A. Advances in pharmaceutical technology, Chapter 4: Solubility parameters for prediction of drug/polymer miscibility in hot-melt extruded formulations. United Kingdom: John Wiley & Sons Ltd; 2012.

46. Silverstein RM, Bassler GC, Morril TC. Spectrometric identification of organic compounds. New York: Wiley; 1991. p. 91–131.

47. Al-Obaidi H, Buckton G. Evaluation of griseofulvin binary and ternary solid dispersions with HPMCAS. AAPS PharmSciTech. 2009;10(4):1172–7.

48. Shah N, Iyer RM, Mair HJ, Choi DS, Tian H, Diodone R, et al. Improved human bioavailability of vemurafenib, a practically insoluble drug, using an amorphous polymer-stabilized solid dispersion prepared by a solvent-controlled coprecipitation process. J Pharm Sci. 2013;102(3):967–81.

49. Pirayavaraporn C, Rades T, Tucker IG. Determination of moisture content in relation to thermal behavior and plasticization of Eudragit RLPO. Int J Pharm. 2012;422:68–74.

50. Sarode AL, Obara S, Tanno FK, Sandhu H, Iyer R, Shah N. Stability assessment of hypromellose acetate succinate (HPMCAS) NF for application in hot melt extrusion (HME). Carbohydr Polym. 2014;101:146–53.